mained negative to the test potential. Under these conditions, $GABA_A$ receptor activation produced a larger $Cl^-$ flux, and acetazolamide induced a −18-mV shift in the reversal potential toward $E_{Cl}$ ($n$ = 4).
25. M. L. Mayer and G. L. Westbrook, *J. Physiol. (London)* **394**, 501 (1987).
26. L. Vyklicky Jr., V. Vlachova, J. Krusek, *ibid.* **430**, 497 (1990); S. F. Traynelis and S. G. Cull-Candy, *ibid.* **433**, 727 (1991).
27. $GABA_B$ antagonists enhance long-term potentiation (LTP) induction by high-frequency stimulation [C. H. Davies and G. L. Collingridge, *Pharmacol. Commun.* **2**, 98 (1992)], whereas $GABA_B$ agonists enhance LTP induction by lower frequency stimulation [D. D. Mott and D. V. Lewis, *Science* **252**, 1718 (1992); C. H. Davies, S. J. Starkey, M. F. Pozza, G. L. Collingridge, *Nature* **349**, 609 (1992)].
28. D. M. Woodbury and J. W. Kemp, in *Antiepileptic Drugs*, D. M. Woodbury and J. K. Penry, Eds. (Raven Press, New York, 1982), pp. 771–789.
29. M. A. Whittington, R. D. Traub, J. G. R. Jeffreys, *Nature* **373**, 612 (1995); H. B. Michelson and R. K. S. Wong, *J. Physiol. (London)* **477**, 35 (1994).
30. R. L. Smith, G. H. Clayton, C. L. Wilcox, K. W. Escuerdo, K. J. Staley, *J. Neuroscience*, **15**, 4057 (1995).
31. M. J. During *et al.*, *Nature* **376**, 174 (1995).
32. A. L. Hodgkin and B. Katz, *J. Physiol. (London)* **108**, 37 (1949).
33. The small, late outward component that is not affected by amiloride and acetazolamide is due to diffusion of muscimol toward somatic $GABA_A$ receptors, where the $Cl^-$ gradient is more stable (*12, 19, 22*).
34. We thank T. Dunwiddie and R. Nicoll for helpful comments on the manuscript. Supported by NIH grants (NS01573, HD27827, and AA03527) and the American Epilepsy Foundation.

10 January 1995; accepted 30 May 1995

# Recurrent Excitation in Neocortical Circuits

Rodney J. Douglas,* Christof Koch, Misha Mahowald, Kevan A. C. Martin, Humbert H. Suarez†

**The majority of synapses in the mammalian cortex originate from cortical neurons. Indeed, the largest input to cortical cells comes from neighboring excitatory cells. However, most models of cortical development and processing do not reflect the anatomy and physiology of feedback excitation and are restricted to serial feedforward excitation. This report describes how populations of neurons in cat visual cortex can use excitatory feedback, characterized as an effective "network conductance," to amplify their feedforward input signals and demonstrates how neuronal discharge can be kept proportional to stimulus strength despite strong, recurrent connections that threaten to cause runaway excitation. These principles are incorporated into models of cortical direction and orientation selectivity that emphasize the basic design principles of cortical architectures.**

The basic functional architecture of the neocortex, which forms 70 to 80% of the primate brain, is now well established: Neurons with similar functional properties are aggregated together, often in columns or swirling, slab-like arrangements. This architecture reflects the fact that, although lateral connections do occur between and across columns (*1*), most connections are made locally within the neighborhood of a 1-mm column, as Hubel and Wiesel (*2*) originally suggested (*3*).

The neocortex is dominated by excitatory connections. Eighty-five percent of synapses within the gray matter are excitatory and most of these synapses originate from cortical neurons (*4*). Moreover, about 85% of the 5000 to 10,000 synapses made by excitatory neurons are onto other excitatory neurons (*4, 5*), which suggests that excitatory corticocortical synapses must contribute strongly to the response characteristics of individual neurons. This view is in agreement with electrophysiological findings (*6*). In interpretations of cortical function, however, feedback excitation has been almost completely neglected in favor of a simple feedforward view (*2, 7*). But we now know, on the basis of anatomical evidence, that feedforward excitation from subcortical structures is not prominent: In the primary visual cortex of cats and primates, connections arising from the lateral geniculate nucleus (LGN) make up less than 10% of excitatory synapses formed with the input neurons of cortex layer IV spiny stellate cells (*8*). Most synapses onto spiny stellate cells originate from layer VI pyramids and other spiny stellate cells (*9*).

Given this massive excitation, which has been proposed to be a basic feature of cortical operation (*10*), can we infer the fraction of neurons that make first-order recurrent or reciprocal connections, in which two neurons directly excite each other (*11*)? We estimated the number of such recurrent connections for the spiny stellate cells of layer IV in the cat visual cortex from our detailed three-dimensional (3D) reconstructions of the axons and maps of the synapses they receive (*9*). The boutons of these cells usually occur in a few clusters (*12*). Approximation of the radial density of synaptic boutons in the cluster surrounding the soma by a 3D Gaussian distribution (characterized by its standard deviation $\sigma$; Fig. 1A) enables straightforward computation of the fraction of synapses onto a spiny stellate cell in layer IV (Fig. 1B). Even when we only consider synapses within this primary cluster, recurrent connections among spiny stellate cells can provide a significant source of recurrent excitation.

The electronic circuit analogy of Fig. 2A illustrates how recurrently connected neurons amplify current (*13*). The current-discharge curve of a single representative neuron shows that the discharge frequency is proportional to the excitatory current delivered to the soma. Discharge is represented by voltage in the electronic model; here a conductance G (the value of which is inversely related to the slope of the current-discharge curve) will yield the discharge relation of a hypothetical linear neuron. The neuron's firing frequency $F$ corresponds to the voltage across the conductance induced by the total current reaching the "soma" in our simple model of a neuron.

The simplest case of recurrent excitation occurs in a population of identical neurons all receiving the same feedforward input current $I_{ff}$ and forming identical synapses with each other. Any one neuron within this population contributes some excitatory current to each of its neighbors in the population and receives from all of them a recurrent feedback component $I_{rec}$. As a simple model of synaptic interaction, we assume that the current that flows into a neuron from an excitatory synapse is proportional to the discharge frequency of the presynaptic cell. Because all synapses and neurons are assumed to be identical, we can reduce this network to a single neuron that receives a recurrent current $I_{rec}$ proportional to its own firing frequency $F$. This lumped recurrent synapse behaves as a voltage-controlled current source with an amplitude of $\alpha F$, where $\alpha$ is the excitatory conductance. We can think of $\alpha$ as a phenomenological "network conductance" because it is generated by the activity of the network of neurons. At equilibrium, the firing rate of the network $F^*$ must obey

$$I_{ff} + \alpha F^* = GF^* \quad (1)$$

(Fig. 2B). Thus, the output of the popula-

R. J. Douglas, Institute of Neuroinformatics, University and Eidgenössische Technische Hochschule, Zürich 8006, Switzerland; Computation and Neural Systems Program, 139-74, California Institute of Technology, Pasadena, CA 91125, USA; and Center for Biological and Medical Systems, Imperial College, London SW7 ZBT, UK.
C. Koch and H. H. Suarez, Computation and Neural Systems Program, 139-74, California Institute of Technology, Pasadena, CA 91125, USA.
M. Mahowald, Institute of Neuroinformatics, University and Eidgenössische Technische Hochschule, Zürich 8006, Switzerland, and Center for Biological and Medical Systems, Imperial College, London SW7 ZBT, UK.
K. A. C. Martin, Medical Research Council Anatomical Neuropharmacology Unit, Oxford OX1 3TH, UK.

*To whom correspondence should be addressed.
†Present address: Lancet Online Corporation, Kendall Square, Cambridge, MA 02139, USA.

Downloaded from www.sciencemag.org on March 12, 2013

tion is proportional to the feedforward input current, according to the expression

$$F^* = \frac{I_{ff}}{G - \alpha} \quad (2)$$

If $G > \alpha$, the recurrent excitation within the population is stable in the sense that it remains bounded without the restraint of saturation. In electrical engineering terms, the open loop gain, $\alpha/G$, in this case is less than 1. By contrast, the amount by which the circuit amplifies $I_{ff}$, the closed loop or system gain,

$$\frac{\partial(I_{ff} + I_{rec})}{\partial I_{ff}} = \frac{G}{G - \alpha} \quad (3)$$

can be much greater than 1. As $\alpha$ approaches G, the total input current is mainly attributable to the recurrent current $I_{rec}$ rather than the feedforward current $I_{ff}$ and the response of the system becomes dominated by the contribution of the recurrent pathway. If $\alpha > G$, the open loop gain exceeds 1 and there is no equilibrium. A small change in total input current generates a recurrent current that exceeds the original change and so the system diverges until it is driven into saturation.

What is the open loop gain for current amplification within a population of stellate cells? Adapted cortical neurons have a current-discharge relation that is linear over the first nanoampere, with a slope of 100 spikes per second per nanoampere to the nearest order of magnitude. Thus, G is 10 pA per spike per second. Values of $\alpha$ are calculated from the current delivered by each excitatory synapse and the number of recurrent excitatory synapses. Each synapse provides roughly 0.1 pA per spike per second (*14*). Figure 1B shows that neurons with bouton distributions of $\sigma = 100$ μm would make 117 first-order recurrent connections with as many neighbors, which implies that $\alpha$ is 11.7 pA per spike per second in this case. Because $\alpha > G$ the open loop gain is greater than 1, and in the absence of inhibition, the population of cells would reach their maximal discharge rate. Removal of the initial stimulus, the feedforward LGN input, would have no effect on the subsequent activity because the recurrent excitation alone is sufficient to keep the population active (*13*, *15*).

Visual cortical neurons do not exhibit this bistability; for example, they respond proportionally to changes in contrast (*16*). Proportional behavior can be achieved by controlling the recurrent amplification with small amounts of feedforward or feedback inhibition that affect the open loop gain. If the feedback inhibitory synapse is approximated as a current source with an amplitude of $\beta F$, then $\beta$ acts as an inhibitory network conductance of the opposite sign to the excitatory network conductance. Under these conditions, the total recurrent current arriving at the soma is given by $I_{rec} = (\alpha - \beta)F$, with a steady-state firing frequency $F^*$ given by $I_{ff} + (\alpha - \beta)F^* = GF^*$ (Fig. 2B) and an amplification factor of $1/(G + \beta - \alpha)$. The feedback inhibition mediated by linear synapses acts as a multiplicative, shunting-like inhibition that changes the gain of the cortical response to a given input current (Fig. 2B), whereas linear feed-

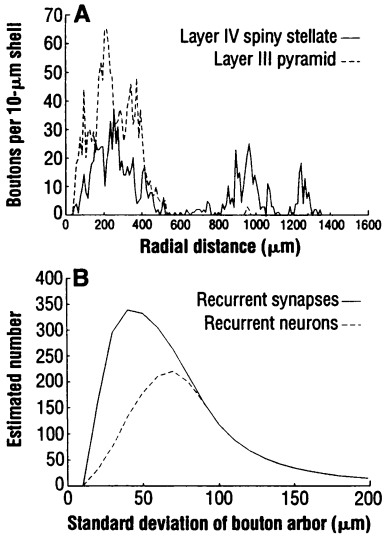


**Fig. 1.** Recurrent synaptic connections between spiny neurons in cat visual cortex. (**A**) Radial density of synaptic boutons as a function of the distance from the cell body of two cells, a layer IVA spiny stellate and a layer II–III pyramidal neuron. In both cases, the axons could not be completely reconstructed and the total number of boutons is underestimated. Nevertheless, the data show that the primary cluster of boutons extends from the soma to a distance of about 500 μm. The primary bouton clusters of these cells can be described by a spherical Gaussian distribution with $\sigma$ between 100 and 120 μm. Data were obtained by computer-assisted reconstruction of neurons in cat striate cortex that had been labeled with horseradish peroxidase during the course of physiological experiments in vivo. (**B**) Numerical estimate of the number of first-order recurrent connections made within the primary cluster of a spiny stellate neuron, and of the number of neighboring spiny stellate neurons that participate in these recurrent connections as a function of the standard deviation $\sigma$ of the axonal tree. For clusters with $\sigma = 100$ μm, spiny stellate cells receive 117 recurrent connections from as many neighbors. For $\sigma = 150$ μm, there are only 34 recurrent connections. The following parameters, drawn from the literature and our own data, were used to calculate these estimates: $4 \times 10^4$ spiny stellate cells per cubic millimeter, $6 \times 10^8$ asymmetrical (excitatory) synapses per cubic millimeter, and 5000 total synapses on the soma and dendrites of stellate cells (of which 1200 derive from other stellates). No excitatory synapses are made within 10 μm of the somata of spiny stellate cells. Five thousand synapses are made by the axonal arbor (of which 1200 are made onto other stellate cells). We assumed that one-third of the boutons occur in the primary cluster and that they are homogeneously distributed in 3D space.

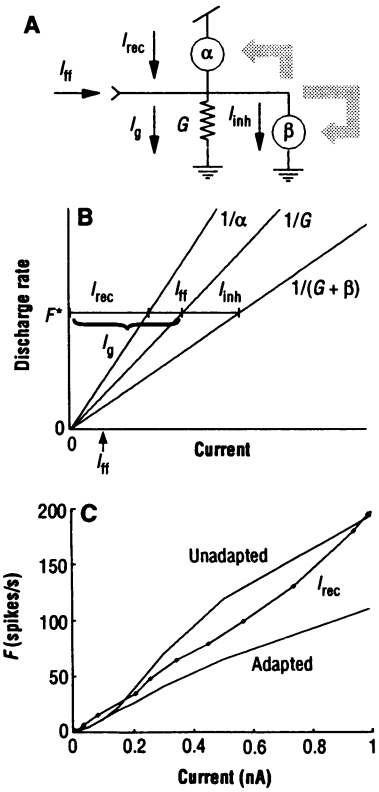


**Fig. 2.** Current amplification by recurrently connected neurons. (**A**) An electronic equivalent circuit for a discharging cortical neuron embedded in its recurrent network. $I_g$ denotes the current dissipated by the spike discharge mechanism, which is assumed to be linear and characterized by conductance *G*. Recurrent excitation generates an effective "network conductance" $\alpha$, which is represented in the schematic as a current source that is controlled (gray arrow) by the output voltage across *G* (that is, by the firing frequency of the neuron). Recurrent inhibition generates another network conductance, $\beta$. The effective conductance of the neuron is thus $G_{eff} = G + \beta - \alpha$. (**B**) Current-discharge relations characterizing the behavior of the cortical amplifier. The $1/G$ line, corresponding to the current-discharge curve, expresses the amount of current $I_g$ dissipated across the somatic membrane by spike currents at discharge rate *F*. The $1/(G + \beta)$ curve indicates the increased current, $I_g + I_{inh}$, required to maintain a given discharge rate in the presence of inhibition that is proportional to the output of the neurons. The $1/\alpha$ curve expresses the dependence of the excitatory feedback current $I_{rec}$, measured in a particular neuron, on the average output rate of neurons in the population. For any particular input current $I_{ff}$, the steady-state discharge rate $F^*$ occurs where the equation $I_{rec} + I_{ff} = I_g + I_{inh}$ is satisfied. At $F^*$ the input current $I_{ff}$ is exceeded in amplitude by the recurrent current $I_{rec}$. (**C**) Adapted (A) and unadapted (UA) current-discharge curves and feedback current $I_{rec}$ for a population of realistic pyramidal neurons modeled by computer simulations (*17*). The adapted current-discharge and the recurrent current relation are approximately linear. Because the adapted current-discharge curve does not cross $I_{rec}$ and the two curves diverge away from each other, the network acts as a proportional amplifier.

Downloaded from www.sciencemag.org on March 12, 2013

forward inhibition acts more like an offset that reduces the input current $I_{in}$ by a given amount.

Even in the absence of inhibition, proportional amplification may be imposed by the intracortical arborization of the axonal tree of the spiny stellate cells. Figure 1B shows that recurrence (and hence the open loop gain) falls off steeply with σ. For example, neurons with a bouton distribution σ = 150 μm make 34 first-order recurrent connections with 34 neighboring stellate cells. Under these circumstances, α falls to 3.4 pA per spike per second, the open loop gain of recurrent excitation is less than 1, and the circuit provides stable current amplification. Although these numerical estimates of the open loop gain are hypothetical, the spatial extent of the axonal tree may be an important factor in determining the amplitude of the feedback.

We evaluated the performance of the recurrent excitation model against experimental results by modeling direction-selective neurons in a patch of cat striate cortex (*17*, *18*). Our aim was not to study direction selectivity per se, but rather to confirm the principles described above in the context of a simple cortical operation with realistic, spiking neurons. The network in our model consists of 40 excitatory (pyramidal) neurons and 10 inhibitory (smooth) neurons (*19*). Members of the pyramidal population are interconnected by excitatory synapses, but for simplicity the inhibitory neurons provide feedforward inhibitory synapses only. Each neuron comprises a somatic compartment containing the standard complement of voltage-dependent membrane conductances found in cortical cells, and three or four passive dendritic compartments. The spike discharge of the pyramids adapts within 50 ms. The smooth neurons are nonadapting (*20*).

Figure 2C shows the current-discharge curves for the pyramidal cells as well as the recurrent current, $I_{rec}$, as a function of the average discharge rate of the pyramidal population. Because $I_{rec}$ does not intersect the adapted current-discharge curve, the network does not show hysteretic behavior but rather relaxes to its resting state when the input is withdrawn. Moreover, because the $I_{rec}$ curve diverges from the adapted current-discharge curve, the neurons will amplify their input in a proportional manner (*13*). The feedforward input signal to the cortical cells arises from the LGN, whose neurons exhibit little directional preference. Cortical direction selectivity depends on a spatial offset between the LGN inputs to pyramidal and smooth cells (*21*, *22*). In the preferred direction, excitation precedes inhibition, which allows the neurons to begin discharging; in the null direction, excitation and feedforward inhibition overlap temporally and cancel each other.

In a purely feedforward model, feedforward inhibition must be powerful in the null direction to suppress the strong excitation, which must be provided solely by the LGN input. Our simulations (Fig. 3B) confirm that this inhibition should be associated with large changes in the somatic input conductance that would be almost entirely visible from the soma (*23*). Yet direct intracellular measurements have shown that such large shunting changes in conductance do not occur (*24*). The paradox of massive excitation and inhibition in the preferred direction but only small inhibition in the null direction is resolved within the framework of current amplification by cortical circuits. In the preferred direction, the small LGN excitation is large enough to bring the pyramidal cells above their firing threshold. In the model outlined above, within 100 ms the recurrent current is 4.7 times the effective input current (Fig. 3C). The amplified input elicits a brisk discharge from the neuron. In the null direction, the small LGN excitation overlaps in time with feedforward inhibition and the cell remains silent. This small amount of inhibition produces only small changes in the somatic input conductance (Fig. 3A).

Iontophoretic application of bicuculline, a selective antagonist of γ-aminobutyric acid A ($GABA_A$) receptors, leads to a significant reduction or even outright elimination of direction selectivity in simple cells in cat striate cortex (*21*). We obtained analogous results with our model (*17*). In an elaboration of Sillito's experiments, Nelson *et al.* (*25*) blocked $GABA_A$ and $GABA_B$ receptors intracellularly in a single neuron. They found that direction selectivity was reduced, but did not disappear, in this cell. The same result holds for our model (Fig. 3D), because the major fraction of the excitatory current in a single GABA-blocked neuron derives from other cortical cells whose direction selectivity is unaffected.

Despite the amplification inherent in our recurrent excitation model, it reproduces the linear behavior reported by Jagadeesh *et al.* (*26*). They observed that the intracellular potential in simple cells in response to a moving sinusoidal grating is accurately predicted by the sum of the membrane re-

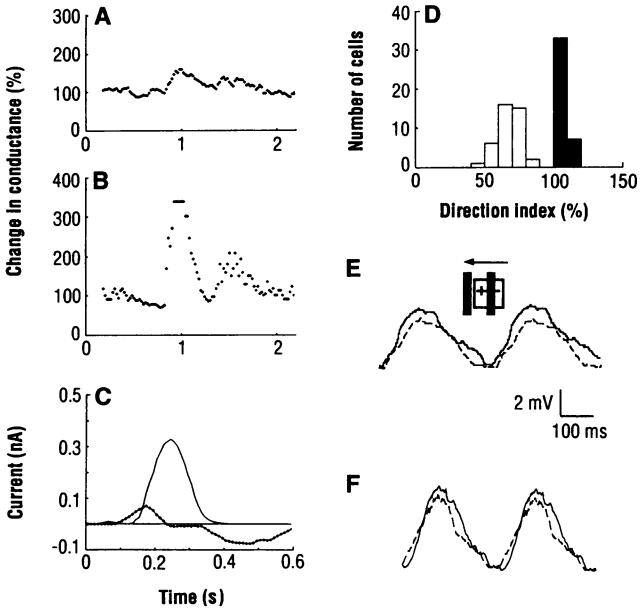


**Fig. 3.** Tests of recurrent excitation in a computer model of a population of direction-selective pyramidal cells. (**A**) Percentage change from baseline somatic input conductance during stimulation by a bar (visual stimulus) moving in the null direction in the feedback model, compared with a purely feedforward model (**B**). Conductance is measured by injecting hyperpolarizing current. The response of the feedback model depends on amplification of the small excitatory feedforward input from LGN afferents. This feedforward input current can be controlled with a moderate inhibitory conductance change, in agreement with experimental data (*24*). The purely feedforward model receives strong excitatory input current from the LGN. The control of this large current requires a large inhibitory conductance change. (**C**) The recurrent excitatory current (solid curve) generated during preferred stimulation, compared with the net input current (dotted curve; the difference between excitatory current from the LGN and feedforward inhibitory current). In this example, the net feedforward input current is amplified by about 4.7 to yield the total excitatory current. (**D**) Histogram of direction selectivity indices of all pyramidal neurons in the normal population (solid bars), compared with the case when inhibition is blocked in a single pyramidal cell (done consecutively for all cells; open bars). Direction selectivity is diminished, but not lost, in agreement with experimental data (*25*). (**E** and **F**) Jagadeesh *et al.* (*26*) applied a "linearity" test by comparing the modulations of somatic membrane potential of a direction-selective cell in response to a drifting sine-wave grating (1 cycle per degree, 2 degrees per second) (solid line) to the response predicted by summation of the modulations evoked by stationary contrast reversal gratings at eight different spatial phases (dashed line). Cells in cat visual cortex [modified from (*26*)] (E) and in the model (F) pass this test, which implies that a network with massive feedback can, under certain limited conditions, behave linearly. Each modulation is the average of the membrane potential over 56 grating cycles. The same median filter was used in both cases to remove action potentials.

Downloaded from www.sciencemag.org on March 12, 2013

sponses to eight spatially displaced stationary gratings (Fig. 3E). This seemingly linear behavior was also obtained in our model (Fig. 3F); it is partly explained by the nature of the stimulus (*27*) and partly by the spike conductances sinking much of the excess current that would otherwise show up as nonlinear contributions to the membrane potential (*17*). This model demonstrates that realistic recurrent cortical circuits can achieve proportional amplification and stability, and that their directional behavior agrees with sophisticated intracellular data. The same principles of recurrent excitation have been used in models of cortical orientation tuning (*28*).

The computational significance of recurrence is well illustrated by the orientation case, because in that problem the current gain experienced by each neuron depends not on a single homogeneous value of $\alpha$ (as described in Fig. 2A) but on the time-dependent network conductances arising out of the excitatory and inhibitory feedback, $\Sigma\alpha_{ij}(t)$ and $\Sigma\beta_{ij}(t)$, from cortical cells responding to different orientations (here the sum is taken over all connections among neurons $i$ and $j$). The variable gain and active thresholding that arise out of these couplings enable the network to enhance noisy incoming signals in the following way. When a noisy input signal is presented to an orientation-selective population of cortical cells (Fig. 4A), the gains of the individual pyramidal neurons are at first equal to each other because their outputs are randomly correlated. The incoherent outputs of the pyramidal neurons are averaged by the inhibitory interneurons, which provides an effective threshold across the pyramidal cells. This threshold has the effect of uncoupling the pyramidal neurons as some members of the population that receive only weak input fall silent. That effect increases the relative $\alpha_{ij}$ between the surviving pyramids, and their gains remain high or increase while the gain of isolated firing neurons falls. The increased output of the survivors enables them to increase the inhibitory threshold, thereby improving the correlation in activity of the active neurons, and so on. Initially the inhibition is subtractive in quality because it is the average over incoherent pyramidal activity. But as the computation converges, the inhibition becomes divisive because its effect on the surviving pyramids is better correlated with their discharge and the inhibitory network conductance (see $\beta$ above) is expressed.

Overall, the population of neurons cooperatively restores the incoming stimulus toward a pattern that is latent in the recurrent connectivity; this permits meaningful outputs to be extracted from incomplete or noisy input patterns by means of variable thresholding followed by amplification (Fig. 4B) (*29*). This restoration is related to recall in content addressable (associative) memories composed of sigmoidal neurons (*15*). However, those networks typically have very strong positive feedback and many stable attractors, whereas the cortical circuits presented here operate in a domain where they can represent in a proportional manner various aspects of the input, such as its contrast or velocity. Functionally, the recurrent cortical architecture combines aspects of analog signal processing ("smart" amplification) with digital signal processing (signal restoration). Similar circuits are likely to explain receptive field properties in other sensory areas. The high degree of cortical interconnectivity, compared to the small number of extracortical inputs, raises the possibility that receptive field properties are not so much determined by the specific patterns of thalamic afferents but are shaped by the collective behavior of large populations of cortical cells. If so, the cortex would represent a substantially richer modifiable architecture than standard feedforward models (*30*).

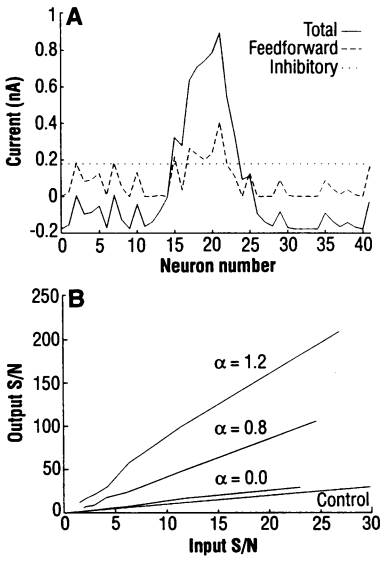


**Fig. 4.** Signal restoration by recurrent excitation. A second, more simplified, model network comprises 42 excitatory and 7 inhibitory "neurons" of the kind described in Fig. 2, A and B. The excitatory neurons are coupled to each other by excitatory connections falling off as a Gaussian distribution (with a $\sigma$ equivalent to two neurons; circular boundary conditions are used). The inhibitory neurons receive input from overlapping subpopulations of excitatory cells. The synaptic strengths of these connections are also Gaussian ($\sigma = 4$). All inhibitory neurons make synapses onto the excitatory population with uniform strength. The network receives a Gaussian pattern of feedforward input currents from the LGN, and this pattern is degraded by a variable amount of noise. (**A**) Amplification of the noisy feedforward input current [signal-to-noise ratio (S/N) = 1.8, here caused by a very noisy oriented signal] by the recurrent network results in the net output current indicated by the solid line. After convergence, most of the noise is subthreshold, while the positive part of the signal is amplified and restored toward the expected Gaussian distribution. The final inhibitory current (dotted line) is shown as a positive current against which the feedforward LGN input signal is compared. The output of a purely feedforward model (dashed line) is simply that part of the LGN signal that exceeds the inhibitory current without any signal restoration. (**B**) Signal enhancement by recurrent excitation and active thresholding. S/N ratios of feedforward inputs and neuronal output discharges are compared in simulations similar to those described in (A). The line labeled Control indicates the parity expected between input and output S/N in an ideal linear unity gain amplifier. In the absence of recurrence ($\alpha = 0$), simple feedforward inhibitory thresholding of a noisy feedforward excitatory signal provides slight signal enhancement. Increasing feedback excitation ($\alpha$) improves the signal-enhancing properties of the network by a combination of amplification and feedback thresholding that restores the noisy input toward patterns latent in the network connectivity. The thresholding inhibition required is relatively small because small feedforward LGN inputs are amplified.

## REFERENCES AND NOTES


1. C. D. Gilbert and T. N. Wiesel, *J. Neurosci.* **3**, 116 (1983); *ibid.* **9**, 2432 (1989).
2. D. H. Hubel and T. N. Wiesel, *J. Physiol.* **160**, 106 (1962).
3. The majority of synapses must be made relatively close to their source neurons so as to minimize the volume of axonal "wiring" and prevent an explosive growth of cortical volume with increasing cell number [C. Mead, *Proc. IEEE* **78**, 1629 (1990); G. Mitchison, *Trends Neurosci.* **15**, 122 (1992)].
4. V. Braitenberg and A. Schüz, *Anatomy of the Cortex* (Springer-Verlag, Berlin, 1991).
5. Z. F. Kisvarday *et al.*, *Exp. Brain Res.* **64**, 541 (1986); B. A. McGuire *et al.*, *J. Neurosci.* **4**, 3021 (1984).
6. D. Ferster and S. Lindstrom, *J. Physiol.* **367**, 217 (1985); *ibid.*, p. 233; K. L. Grieve and A. M. Sillito, *Exp. Brain Res.* **87**, 521 (1991).
7. P. Heggelund, *Exp. Brain Res.* **42**, 89 (1981); D. Ferster, *J. Neurosci.* **7**, 1780 (1987); *ibid.* **8**, 1172 (1988); R. Maex and G. A. Orban, *Proc. Natl. Acad. Sci. U.S.A.* **88**, 3549 (1991); F. Wörgötter and C. Koch, *J. Neurosci.* **11**, 1959 (1991). More recently feedback inhibition has been incorporated in some models; see M. Carandini and D. J. Heeger, *Science* **264**, 1333 (1994).
8. S. LeVay, *J. Neurosci.* **6**, 3564 (1986); E. L. White, *Cortical Circuits: Synaptic Organization of the Cerebral Cortex* (Birkhäuser, Boston, 1989); A. Peters and B. R. Payne, *Cereb. Cortex* **3**, 69 (1993); A. Peters, B. R. Payne, J. Rudd, *ibid.* **4**, 215 (1994).
9. B. Ahmed *et al.*, *J. Comp. Neurol.* **341**, 39 (1994).
10. R. J. Douglas, K. A. C. Martin, D. Whitteridge, *Neural Comput.* **1**, 480 (1989).
11. We ignore here the effects of higher order recurrent connections that further strengthen our conclusions; see R. E. Traub and R. Miles, *Neuronal Networks of the Hippocampus* (Cambridge Univ. Press, Cambridge, 1991).
12. K. A. C. Martin and D. Whitteridge, *J. Physiol.* **353**, 463 (1984); J. S. Lund *et al.*, *Cereb. Cortex* **3**, 148 (1993); Y. Amir *et al.*, *J. Comp. Neurol.* **334**, 19 (1993).
13. See also H. H. Suarez, thesis, California Institute of Technology (1995) for an analysis of this system's dynamics and the influence of nonlinearities.
14. Ö. Bernander, C. Koch, R. J. Douglas, *J. Neurophysiol.* **72**, 2743 (1994).
15. This kind of feedback network has been studied in the artificial neural network community as the basis for content addressable memory [D. J. Willshaw, O. P. Buneman, H. C. Longuet-Higgins, *Nature* **222**, 960


Downloaded from www.sciencemag.org on March 12, 2013

(1969); D. Marr, *Proc. R. Soc. London Ser. B Biol. Sci.* **176**, 161 (1970); J. J. Hopfield, *Proc. Natl. Acad. Sci. U.S.A.* **81**, 3088 (1984); S. Grossberg, *Neural Networks* **1**, 17 (1988); J. Hertz, A. Krogh, R. G. Palmer, *Introduction to the Theory of Neural Computation* (Addison-Wesley, Redwood City, CA, 1991)].
16. I. Ohzawa *et al.*, *Nature* **298**, 266 (1982).
17. H. H. Suarez, C. Koch, R. J. Douglas, *J. Neurosci.*, in press.
18. R. Maex [thesis, Leuven University, Belgium (1995)] has simulated a similar model of cortical direction selectivity with similar results to ours.
19. The feedforward inputs from the LGN to the cortical pyramidal and smooth neurons were Poisson-distributed spike trains whose instantaneous rate was modulated by the visual stimulus. The stimulus, usually a bar or sinusoidal grating, was convolved with the spatial-temporal receptive field characteristic of the LGN ON relay cells of the X type [J. D. Victor, *J. Physiol.* **386**, 219 (1987)]. Direction selectivity was obtained by spatially offsetting the LGN input to smooth cells by 5′ with respect to LGN inputs to the pyramidal cells. All synapses were modeled as conductances with appropriate reversal potentials, and time courses and amplitudes were compatible with available in vitro data. The synapses provided $GABA_A$ and $GABA_B$ inhibition and non–*N*-methyl-D-aspartate (NMDA) excitation. All data presented here were obtained with a single set of neuronal and network parameters.
20. D. A. McCormick *et al.*, *J. Neurophysiol.* **54**, 782 (1985).
21. A. M. Sillito, *J. Physiol.* **250**, 305 (1975); *ibid.* **271**, 699 (1977).
22. P. O. Bishop, J. S. Coombs, G. H. Henry, *ibid.* **219**, 625 (1971); L. Ganz, R. Felder, *J. Neurophysiol.* **51**, 294 (1984); J. McLean, S. Raab, L. A. Palmer, *Visual Neurosci.* **11**, 271 (1994). We do not here model lagged geniculate cells that might also contribute to direction selectivity [see D. N. Mastronarde, *J. Neurophysiol.* **57**, 357 (1987); A. B. Saul and A. L. Humphrey, *ibid.* **64**, 206 (1990)].
23. C. Koch *et al.*, *J. Neurosci.* **10**, 1728 (1990).
24. Peak measured conductance changes in the null direction are less than 25% of the somatic input conductance [R. J. Douglas, K. A. C. Martin, D. Whitteridge, *Nature* **332**, 642 (1988); *J. Physiol.* **440**, 659 (1991); X. Pei *et al.*, *Neuroreport* **2**, 485 (1991); D. Ferster and B. Jagadeesh, *J. Neurosci.* **12**, 1262 (1992)].
25. S. Nelson *et al.*, *Science* **265**, 774 (1994).
26. B. Jagadeesh *et al.*, *ibid.* **262**, 1901 (1993). See also R. C. Reid, R. E. Soodak, R. M. Shapley, *Proc. Natl. Acad. Sci. U.S.A.* **84**, 8740 (1987).
27. Nonlinear Fourier components in the half-wave rectified responses to gratings tend to cancel out when added with different temporal offsets.
28. D. Somers, S. B. Nelson, M. Sur, *J. Neurosci.*, in press; R. Ben-Yishai, R. Lev Bar-Or, H. Sompolinsky, *Proc. Natl. Acad. Sci. U.S.A.* **92**, 3844 (1995).
29. R. J. Douglas, M. A. Mahowald, K. A. C. Martin, *IEEE Intl. Conf. Neural Networks*, 1848 (1994).
30. J. Allman, F. Miezin, E. McGuiness, *Annu. Rev. Neurosci.* **8**, 407 (1985); B. Gulyas *et al.*, *J. Physiol.* **57**, 1767 (1987); C. D. Gilbert and T. N. Wiesel, *Vision Res.* **30**, 1689 (1990); C. Koch and J. Davis, *Large Scale Neuronal Theories of the Brain* (MIT Press, Cambridge, MA, 1994).
31. We thank the U.S. Office of Naval Research for their long-term support of this work. In addition this work was supported by the Air Force Office of Scientific Research, the Gatsby Foundation, the Medical Research Council, the National Institute of Mental Health, the National Science Foundation, the European Community, the Human Frontiers Science Program, the Wellcome Trust, and the Royal Society. We thank J. Anderson for reconstructions of neurons in cat striate cortex and G. Holt for help with the graphics.

16 February 1995; accepted 5 June 1995

# Object-Centered Direction Selectivity in the Macaque Supplementary Eye Field

C. R. Olson* and S. N. Gettner

**Object-centered spatial awareness—awareness of the location, relative to an object, of its parts—plays an important role in many aspects of perception, imagination, and action. One possible basis for this capability is the existence in the brain of neurons with sensory receptive fields or motor action fields that are defined relative to an object-centered frame. In experiments described here, neuronal activity was monitored in the supplementary eye field of macaque monkeys making eye movements to the right or left end of a horizontal bar. Neurons were found to fire differentially as a function of the end of the bar to which an eye movement was made. This is direct evidence for the existence of neurons sensitive to the object-centered direction of movements.**

Many behaviors and mental processes require the use of spatial information defined in an object-centered reference frame. Visual object recognition, for example, is generally thought to require explicit encoding of the locations of parts relative to the object (*1*). Visually guided motor behavior also depends on object-centered information. The hand, in reaching around an object, must move along a trajectory defined relative to the object. Likewise, the eyes, during scanning, may be directed to a featureless point defined solely by its relation to visible details elsewhere in the scene. Evidence that localized groups of neurons represent specific parts of object-centered space has been provided by studies of visual neglect in humans. In many cases of hemifield neglect, patients overlook features on the contralesional side of a visible object even when the neglected side of the object has been viewed through the good hemifield (*2*). Object-centered neglect must arise from the loss of neurons that mediated awareness of one half of the current reference object rather than one half of visual space or the retina. Such neurons could be expected to have sensory receptive fields or motor action fields defined with respect to the current reference object. Previous single-unit studies have produced only limited evidence for the existence of neurons with these properties (*3*). In this report, we demonstrate that neurons in the supplementary eye field (SEF) of the macaque monkey encode eye-movement direction with respect to an object-centered reference frame.

The SEF is an oculomotor area on the dorsomedial surface of the frontal lobe. Electrical stimulation of the macaque SEF elicits eye movements with complex properties, including dependence on initial orbital position (*4*). Neurons in the SEF discharge preferentially before and during saccades in a restricted range of directions (*5*). Some SEF neurons are selectively active during the learning of associations between visual-pattern cues and eye-movement directions (*6*). These observations suggest that the SEF mediates processes of comparatively high order that are related to oculomotor control.

We prepared two male macaque monkeys for single-unit recording by standard methods (*7*). We mapped out the SEF in both hemispheres of one monkey and in the right hemisphere of the second monkey (*8*). To assess object-centered direction selectivity, we trained the monkeys to perform an oculomotor task in which the object-centered direction of eye movements (to the left or right end of a horizontal target bar) could be dissociated from their orbit-centered direction (leftward or rightward in the orbit). The sequence of events during a representative trial is shown in Fig. 1A. A cue presented early in each trial (a spot superimposed on one end of a sample bar) instructed the monkey to look to the left or right end of the target bar. The target bar subsequently appeared at one of three locations (Fig. 1B). Across eight possible conditions (Fig. 1C), eye-centered direction (leftward or rightward in the orbit) was fully counterbalanced against object-centered direction (to the left or right end of the bar) (*9*).

Twenty-nine neurons in one monkey were studied while the monkey performed this task. The neuron shown in Fig. 2 fired more strongly when the eye movement was to the left end of the target bar (left column) than when it was to the right end (right column). This was true regardless of the orbital direction of the movement (rightward in the first and third rows; leftward in the second and fourth rows). Firing was stronger in bar-left trials, not only during the period between the cue and the

Department of Oral and Craniofacial Biological Sciences, College of Dental Surgery, University of Maryland, Baltimore, MD 21201, USA.

*To whom correspondence should be addressed. E-mail: colson@umabnet.ab.umd.edu

Downloaded from www.sciencemag.org on March 12, 2013